

Characterization of low-resistance ohmic contacts to heavily carbon-doped n-type InGaAsBi films treated by rapid thermal annealing

Shu-Xing Zhou(周书星), Li-Kun Ai(艾立鹍), Ming Qi(齐鸣), An-Huai Xu(徐安怀), Jia-Sheng Yan(颜家圣), Shu-Sen Li(李树森), and Zhi Jin(金智)

Citation: Chin. Phys. B, 2021, 30 (**2**): 027304. DOI: 10.1088/1674-1056/abcf97
Journal homepage: http://cpb.iphy.ac.cn; http://iopscience.iop.org/cpb

What follows is a list of articles you may be interested in

Improved electrical properties of NO-nitrided SiC/SiO_2 interface after electron irradiation

Ji-Long Hao(郝继龙), Yun Bai(白云), Xin-Yu Liu(刘新宇), Cheng-Zhan Li(李诚瞻), Yi-Dan Tang(汤益丹), Hong Chen(陈宏), Xiao-Li Tian(田晓丽), Jiang Lu(陆江), Sheng-Kai Wang(王盛凯)

Chin. Phys. B, 2020, 29 (**9**): 097301. DOI: 10.1088/1674-1056/ab9434

Influence of $Zr_{50}Cu_{50}$ thin film metallic glass as buffer layer on the structural and optoelectrical properties of AZO films

Bao-Qing Zhang(张宝庆), Gao-Peng Liu(刘高鹏), Hai-Tao Zong(宗海涛), Li-Ge Fu(付丽歌), Zhi-Fei Wei(魏志飞), Xiao-Wei Yang(杨晓炜), Guo-Hua Cao(曹国华)

Chin. Phys. B, 2020, 29 (**3**): 037303. DOI: 10.1088/1674-1056/ab6c50

Effects of active layer thickness on performance and stability of dual-active-layer amorphous InGaZnO thin-film transistors

Wenxing Huo(霍文星), Zengxia Mei(梅增霞), Yicheng Lu(卢毅成), Zuyin Han(韩祖银), Rui Zhu(朱锐), Tao Wang(王涛), Yanxin Sui(隋妍心), Huili Liang(梁会力), Xiaolong Du(杜小龙)

Chin. Phys. B, 2019, 28 (**8**): 087302. DOI: 10.1088/1674-1056/28/8/087302

Influence of deep defects on electrical properties of Ni/4H-SiC Schottky diode

Jin-Lan Li(李金岚), Yun Li(李赟), Ling Wang(汪玲), Yue Xu(徐跃), Feng Yan(闫锋), Ping Han(韩平), Xiao-Li Ji(纪小丽)

Chin. Phys. B, 2019, 28 (**2**): 027303. DOI: 10.1088/1674-1056/28/2/027303

Effect of Au/Ni/4H-SiC Schottky junction thermal stability on performance of alpha particle detection

Xin Ye(叶鑫), Xiao-Chuan Xia(夏晓川), Hong-Wei Liang(梁红伟), Zhuo Li(李卓), He-Qiu Zhang(张贺秋), Guo-Tong Du(杜国同), Xing-Zhu Cui(崔兴柱), Xiao-Hua Liang(梁晓华)

Chin. Phys. B, 2018, 27 (**8**): 087304. DOI: 10.1088/1674-1056/27/8/087304

Characterization of low-resistance ohmic contacts to heavily carbon-doped n-type InGaAsBi films treated by rapid thermal annealing*

Shu-Xing Zhou(周书星)[1,†], Li-Kun Ai(艾立鹍)[2], Ming Qi(齐鸣)[2], An-Huai Xu(徐安怀)[2], Jia-Sheng Yan(颜家圣)[3], Shu-Sen Li(李树森)[3], and Zhi Jin(金智)[4]

[1] *Hubei Key Laboratory of Low Dimensional Optoelectronic Materials and Devices, Hubei University of Arts and Science, Xiangyang* 441053, *China*
[2] *State Key Laboratory of Functional Materials for Informatics, Shanghai Institute of Microsystem and Information Technology, Chinese Academy of Sciences, Shanghai* 200050, *China*
[3] *Hubei Key Laboratory of High Power Semiconductor Technology, Xiangyang* 441021, *China*
[4] *Institute of Microelectronics, Chinese Academy of Sciences, Beijing* 100029, *China*

(Received 4 November 2020; revised manuscript received 25 November 2020; accepted manuscript online 2 December 2020)

Carbon-doped InGaAsBi films on InP:Fe (100) substrates have been grown by gas source molecular beam epitaxy (GSMBE). The electrical properties and non-alloyed Ti/Pt/Au contact resistance of n-type carbon-doped InGaAsBi films were characterized by Van der Pauw–Hall measurement and transmission line method (TLM) with and without rapid thermal annealing (RTA). It was found that the specific contact resistance decreases gradually with the increase of carrier concentration. The electron concentration exhibits a sharp increase, and the specific contact resistance shows a noticeable reduction after RTA. With RTA, the InGaAsBi film grown under CBr_4 supply pressure of 0.18 Torr exhibited a high electron concentration of 1.6×10^{21} cm^{-3} and achieved an ultra-low specific contact resistance of 1×10^{-8} Ω·cm^2, revealing that contact resistance depends greatly on the tunneling effect.

Keywords: InGaAsBi, electrical properties, contact resistance, rapid thermal annealing

PACS: 73.40.Mr, 68.35.bg, 68.35.Ct, 85.30.De **DOI:** 10.1088/1674-1056/abcf97

1. Introduction

For the increased scaling of InP terahertz devices such as InP heterojunction bipolar transistors (HBTs) and high electron mobility transistors (HEMTs) for high-speed communications,[1,2] ultra-low resistance metal-semiconductor ohmic contacts with shallow diffusion depths and minimal lateral penetration are very important.[3–6] Usually, heavily silicon-doped InGaAs cap layers have been used as contact layers to achieve low contact resistance fabricated by *ex situ* or *in situ* non-alloyed contacts in InP HEMTs[7–9] and HBTs.[10–12] The efficacy of high silicon-doping concentrations in InGaAs cap layers to obtain contact resistance of 4×10^{-8} Ω·cm^2 has been demonstrated because the use of high semiconductor doping concentrations is known to promote current transport due to the tunneling effect.[13–15] However, it is difficult to further reduce the contact resistance by increasing the silicon-doping concentration in InGaAs, which can only be doped to the 19th power owing to the doping solubility limit. Further efforts are needed to reduce contact resistance, such as fine-tuning of surface preparation procedures and various alloy-contact selection.[16]

It has been recently reported that dilute InGaAsBi, lattice-matched to InP, is promising to be used as a contact material for InP terahertz devices because of its higher doping solubility limit[17,18] and narrower band gap compared with InGaAs[19,20] by virtue of bismuth being a very heavy and large atom and the valence band anticrossing (VBAC).[21–23] The author's previous work has first proved that bismuth incorporation into InGaAs induces extremely high n-type carbon-doped InGaAsBi films, and its carrier concentration can exceed 10^{21} cm^{-3}, which is almost two orders of magnitude higher than the doping concentration of silicon in InGaAs.[18] It implies that a lower specific contact resistance of InGaAsBi can be obtained than that of InGaAs according to the tunneling effect.[24]

To fully make use of its potentials for high-speed electronics device fabrication, we have investigated the electrical properties and contact resistance of n-type carbon-doped InGaAsBi films with and without rapid thermal annealing (RTA). With RTA, the electron concentration has a sharp increase, and the specific contact resistance shows a noticeable reduction. An ultra-low specific contact resistance of 1×10^{-8} Ω·cm^2 is observed after RTA, and the corresponding electron concentration is 1.6×10^{21} cm^{-3}. To the best of the authors' knowledge, this is the highest reported room-temperature electron concentration for n-type III–V semiconductor materials to date.

*Project supported by the National Natural Science Foundation of China (Grant Nos. 11705277 and 61434006) and the Project of Hubei University of Arts and Science (Grant No. XK2019053).

†Corresponding author. E-mail: sxzhou@mail.ustc.edu.cn

© 2021 Chinese Physical Society and IOP Publishing Ltd

2. Experimental details

A series of ∼ 500 nm thick n^+ carbon-doped InGaAsBi films were grown on (100) semi-insulating InP substrate using a V90 gas source MBE system. The 7N-purity elemental Ga, In, and Bi were used as the group-III and group-V sources. The arsenic and carbon beams were obtained by thermal cracking of arsine (AsH_3) and carbon tetrabromide (CBr_4) at 1000 °C and 70 °C, separately. The growth rates for $In_{1-y}Ga_yAs_{1-x}Bi_x$ ($y \sim 0.5$) epilayer and $In_{0.53}Ga_{0.47}As$ buffer layer were approximately 1 μm/h. Samples were grown at 275 °C under different CBr_4 supply pressures of 0.18, 0.15, 0.12, 0.09, 0.06, and 0.03 Torr, respectively. Growth details can be found in Ref. [18]. Hall-effect measurements with indium dots as ohmic contacts located on the sample periphery were performed to measure the electronic transport properties of these samples taken from half of the wafer. The portion of the wafer coated with Ti/Pt/Au (15 nm/15 nm/270 nm) by an electron beam evaporation was processed into transmission line model (TLM) structures for contact resistance measurement, as shown in Fig. 1. After processing, the TLM pattern lengths and widths were verified with a scanning electron microscope (SEM). The SEM image of the TLM pattern with mesa etching is shown in Fig. 2. The TLM pattern lengths and widths are about 100 μm and 150 μm, respectively. The contact separations were from 4 μm to 32 μm. The contact resistance was determined by TLM and a four-point (Kelvin) probe technique and measured using an Agilent 4155C semiconductor parameter analyzer. The RTA process was carried out at 200 °C for 2 min in an atmosphere of nitrogen.

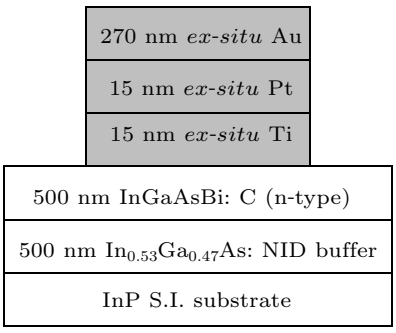


Fig. 1. Cross-section schematic of the metal–semiconductor contact layer structure used for TLM measurement. Ti/Pt/Au (15 nm/15 nm/270 nm) is deposited by an electron beam evaporation.

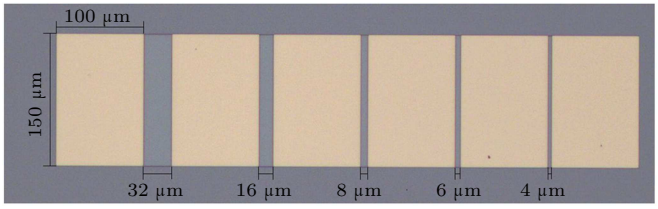


Fig. 2. A microscope image of the TLM pattern used for the contact resistivity (ρ_c) measurement, with contact width $W = 150$ μm.

3. Results and discussion

3.1. Electrical properties

Figure 3 shows the dependence of carrier concentration and mobility on CBr_4 supply pressure for n-type InGaAsBi grown at 275 °C in previous work[18] and n-type InGaAsBi annealed at 200 °C for 2 min duration in this work. As shown in Fig. 3, both the net electron concentrations of as-grown and annealed C-doped InGaAsBi films increase almost linearly with the CBr_4 supply pressure. It has been found that the electron concentration of n-type InGaAsBi films increases sharply and saturates at a maximum concentration of 1.6×10^{21} cm^{-3} under the CBr_4 supply pressure of 0.18 Torr is achieved after annealing at 200 °C for 2 min duration. It is higher than the reported electron concentration to date for n-type III–V semiconductor materials.[25–27] An apparent increase in the electron mobility was observed for the annealed C-doped InGaAsBi films with the carrier concentration lower than 10^{19} cm^{-3}, and when the carrier concentration is greater than 10^{19} cm^{-3}, the mobility has no obvious improvement. As-annealing treatment eliminates defects and improves the electrical properties of carbon-doped InGaAsBi films and, meanwhile, drives more C onto group-III sites as donors, which increases the electron concentration and mobility.[18] A possible mechanism is that as-annealing treatment eliminates Bi-related defects,[28–30] drives more Bi onto group-V sites, and increases the number of activated carbon donors by forming C–Bi bonds around the Bi-related defects.[18] Besides, a self-compensation and the incorporation of the carbon atoms in interstitial sites may also be part of the reasons.

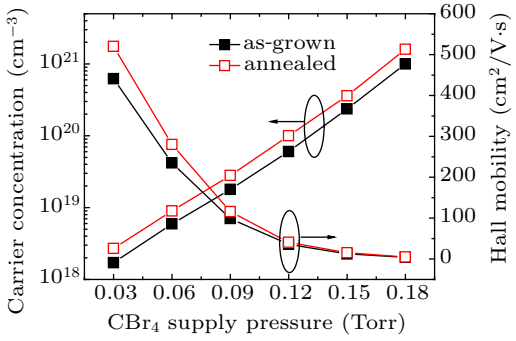


Fig. 3. Dependence of carrier concentration and mobility on CBr_4 supply pressure for as-grown and annealed C-doped InGaAsBi films.

3.2. Contact resistance

Contact resistivities were measured on samples A, B, C, D with four different electron concentrations varying from 1.69×10^{19} cm^{-3} to 1×10^{21} cm^{-3}, and the corresponding CBr_4 supply pressures are 0.09, 0.12, 0.15, and 0.18 Torr, respectively. Resistance measurements were taken both before and after sample annealing in an N_2 environment at 200 °C for 2 min. Figure 4 shows the measured resistivity versus gap spacing obtained from room-temperature TLM measurements

on the n-type InGaAsBi films using the four-point probe technique. For all four samples with and without annealing, the sheet resistance (R_{sh}) and specific contact resistivity (ρ_c) were extracted from the slope and the y-axis (resistivity) intercept of their corresponding linear fits, respectively, as mentioned in Ref. [31]. Figure 5 shows the R_{sh} values obtained from room-temperature Hall-effect measurements of the samples with and without annealing compared to those extracted from the TLM measurement. All of them are in good agreement. The R_{sh} of the samples with and without annealing decreases with increasing carrier concentration, as expected.

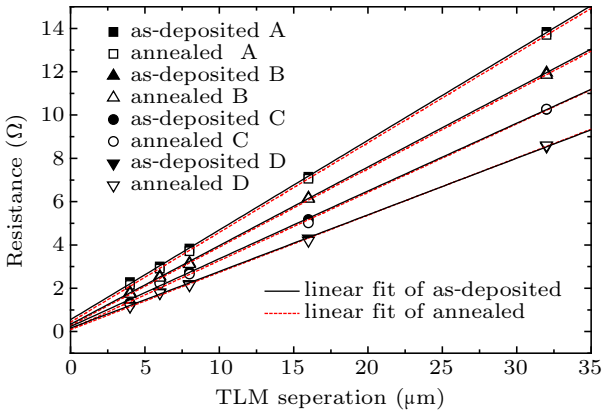


Fig. 4. Measured resistance vs contact separation for the contacts. Contact width is 150 μm. The sheet resistance and contact resistance are calculated from the slope and y-intercept of the line fit.

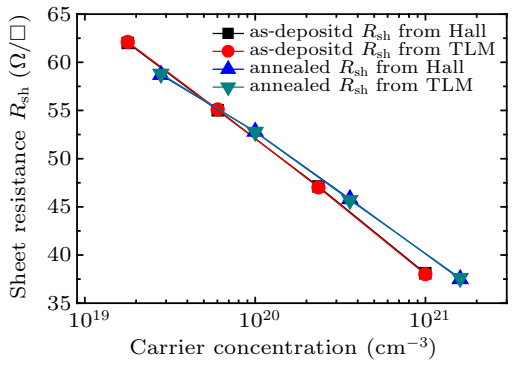


Fig. 5. Sheet resistance versus carrier concentration obtained from room temperature TLM measurements and Hall measurements before and after samples were annealed.

Figure 6 shows the dependence of the specific contact resistance on the carrier concentration for as-deposited and annealed n-type C-doped InGaAsBi films. As shown in Fig. 6, the specific contact resistance decreases gradually with the increase of carrier concentration, revealing that it depends greatly on the doping level. This decrease suggests that the dominant electron transport mechanism is the tunneling effect.[24] It has been found that the specific contact resistance shows a noticeable reduction after RTA, and a minimum specific contact resistance of 1.0×10^{-8} Ω·cm^2 is achieved for the annealed C-doped n-type InGaAsBi film with an electron concentration of 1.6×10^{21} cm^{-3}. We speculate that as-annealing treatment eliminates Bi-related defects in the metal-semiconductor interface and leads to the increase of carrier concentration by activating the inactivated carbon donors mainly by forming C–Bi bonds around the Bi-related defects.[18,28] Additional ionized donors and a shallower depletion at the metal-semiconductor interface exists, thereby reducing the Schottky barrier to electrons and the tunneling resistance, consequently decreasing the contact resistivity.[32]

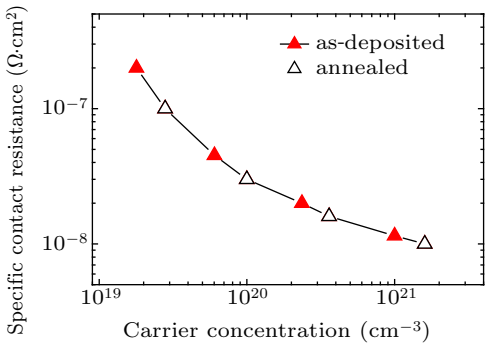


Fig. 6. Specific contact resistance as a function of the carrier concentration for as-deposited and annealed C-doped InGaAsBi films.

3.3. Contact material design

To find the dependence of the specific contact resistance on the carrier concentration and establish which of two epitaxial cap materials (n-InGaAsBi doped by carbon and n-InGaAs doped by silicon) is more advantageous in respect to ohmic contact design, the specific contact resistance as a function of the reciprocal square root of the carrier concentration for annealed Ti/Pt/Au/n-InGaAsBi:C and Ti/Pt/Au /n-InGaAs:Si systems[24] are shown in Fig. 7. The experimental $\ln\rho_c$ vs. $N_d^{-1/2}$ plots presented in Fig. 7 reveals good linearity for both contacts to InGaAsBi and InGaAs, thus supporting the expectation that the field emission is the prevailing current mechanism. According to the tunneling model,[33] $\ln\rho_c$ depends linearly on the reciprocal square root of the doping concentration. The slope of this linearity is determined by $4\pi\phi_{Bn}\sqrt{\varepsilon_s m^*}/h$, where ϕ_{Bn} is the Schottky barrier height, h is the Planck's constant, m^* is the effective mass of the tunneling electron, and ε_s is the semiconductor dielectric constant. The two slopes are approximately equal, indicating that the Schottky barrier heights and dielectric constants for InGaAsBi and InGaAs are roughly the same. It has been demonstrated that a small amount substitution of As with Bi in InGaAs barely impacts the conduction band due to the valence band anticrossing;[20,34] thus, the Schottky barrier height (ϕ_{Bn}) between metal and n-type InGaAsBi remains almost unchanged compared with InGaAs. As shown in Fig. 7, at the same doping concentration, the contact to InGaAs can obtain lower specific contact resistance mainly due to a better surface treatment process. However, the contact to InGaAsBi can achieve the lowest specific contact resistance of 1.0×10^{-8} Ω·cm^2 compared with InGaAs, regardless of the surface treatment process. This is mainly because n-type carbon-doped InGaAsBi

has a higher doping solubility limit to obtain super high n-type doping concentration with more than 10^{21} cm^{-3}. By carefully optimizing surface preparation procedures and various alloy-contact selection, the contact resistance to n-type carbon-doped InGaAsBi can be further reduced. It turns out to be the case that dilute InGaAsBi is suitable to be used as a contact material for InP multi-terahertz devices.

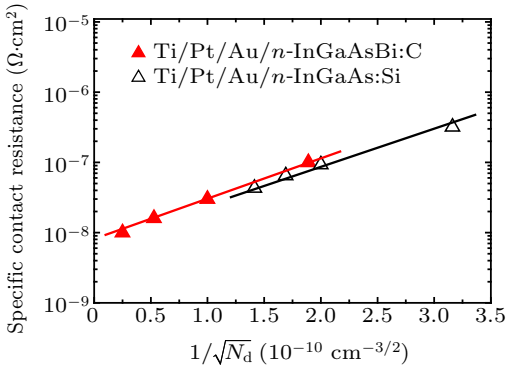


Fig. 7. Specific contact resistance as a function of the reciprocal square root of the carrier concentration (N_d) for annealed Ti/Pt/Au/n-InGaAsBi:C and Ti/Pt/Au/n-InGaAs:Si systems.[24]

4. Conclusion

In summary, we have investigated the effect of rapid thermal annealing on the electrical properties and contact resistance of n-type carbon-doped InGaAsBi films. After RTA, the electron concentration undergoes a sharp increase, and the specific contact resistance shows a noticeable reduction. An annealed n-InGaAsBi film with a carrier concentration of 1.6×10^{21} cm^{-3} exhibited an ultra-low specific contact resistance of 1×10^{-8} Ω·cm^2, revealing that it depends greatly on the doping level. From comparative studies of Ti/Pt/Au contacts to n-InGaAsBi:C and n-InGaAs:Si, it is evident that dilute InGaAsBi is suitable to be used as a contact material for InP multi-terahertz devices.

References

[1] Urteaga M, Griffth Z, Seo M, Hacker J and Rodwell M J W 2017 *Proc. IEEE* **105** 1051

[2] Rode J C, Chiang H W, Choudhary P, Jain V, Thibeault B J, Mitchell W J, Rodwell M, Urteaga M, Loubychev D, Snyder A, Wu Y and Fastenau J M 2015 *IEEE Transactions on Electron Devices* **62** 2779

[3] Baraskar A, Gossard A C and Rodwell M J W 2013 *J. Appl. Phys.* **114** 154516

[4] Lin J C, Yu S Y and Mohney S E 2013 *J. Appl. Phys.* **114** 044504

[5] Baraskar A, Jain V, Lobisser E, Singisetti U, Burek G, Lee Y J, Thibeault B, Gossard A and Rodwell M 2010 *J. Vac. Sci. Technol. B* **28** 517

[6] Uttam S, Mark A, Jeramy D, Brian J, Mark J, Arthur C and Seth R B 2008 *Appl. Phys. Lett.* **93** 183502

[7] Deal W R, Leong K, Radisic V, Sarkozy S, Gorospe B, Lee J, Liu P H, Yoshida W, Zhou J, Lange M, Lai R and Mei X B 2011 *IEEE Microwave & Wireless Components Letters* **21** 368

[8] Tong Z, Ding P, Su Y, Niu J, Wang D and Jin Z 2020 *IEEE Journal of the Electron Devices Society* **8** 600

[9] Zhong Y h, Sun S, Wong W, Wang H, Liu X, Duan Z, Ding P and Jin Z 2017 *Frontiers Inf. Technol. Electronic Eng.* **18** 1180

[10] Rodwell M, Le M and Brar B 2008 *Proc. IEEE* **96** 271

[11] Kashio N, Hoshi T, Kurishima K, Ida M and Matsuzaki H 2014 *IEEE Electron Device Lett.* **35** 1209

[12] Alexandrova M, Flüeckiger R, Lövblom R, Ostinelli O and Bolognesi C R 2014 *IEEE Electron Device Lett.* **35** 1218

[13] Sze S M and Ng K K 2007 *Physics of Semiconductor Devices* 3rd Ed. (Hoboken: John Wiley & Sons)

[14] Baraskar A K, Wistey M, Jain V, Singisetti U, Burek G, Thibeault B, Lee Y, Gossard A C and Rodwell M 2009 *J. Vac. Sci. Technol. B.* **27** 2036

[15] Dormaier R and Mohney S E 2012 *J. Vac. Sci. Technol. B.* **30** 031209

[16] Jain V, Baraskar A K, Wistey M, Singisetti U, Griffith Z, Lobisser E, Thibeault B, Gossard A C and Rodwell M 2009 *IEEE International Conference on Indium Phosphide & Related Materials* pp. 358–361

[17] Dongmo P, Zhong Y, Attia P, Bomberger C, Cheaito R, Ihlefeld J, Hopkins P and Zide J 2010 *J. Appl. Phys.* **112** 093710

[18] Zhou S, Ai L, Qi M, Wang S, Xu A and Guo Q 2018 *J. Mater. Sci.* **53** 3537

[19] Carrier P and Wei S 2004 *Phys. Rev. B* **70** 035212

[20] Kudrawiec R, Kopaczek J, Misiewicz J, Petropoulos J P, Zhong Y and Zide J M O 2011 *Appl. Phys. Lett.* **99** 251906

[21] Alberi K, Wu J, Walukiewicz W, Yu K M, Dubon O D, Watkins S P, Wang C X, Liu X, Cho Y J and Furdyna J 2007 *Phys. Rev. B* **75** 045203

[22] Alberi K, Dubon O D, Walukiewicz W, Yu K M and Krotkus A 2007 *Appl. Phys. Lett.* **91** 051909

[23] Lewis R B, Masnadi-Shirazi M and Tiedje T 2012 *Appl. Phys. Lett.* **101** 082112

[24] Stareev G and Künzel H 1993 *J. Appl. Phys.* **74** 7592

[25] Weyers M, Musolf J, Marx D, Kohl A and Balk P 1990 *J. Cryst. Growth* **105** 383

[26] Xua X G, Giesen C, Xu J, Heuken M and Heime K 1997 *J. Cryst. Growth* **181** 26

[27] Petkos G M, Goodhew P J and Joyce T B 1996 *J. Cryst. Growth* **164** 415

[28] Rodrigo J F, Sales D L, Shafi M, Henini M, Turyanska L, Novikov S and Molina S I 2010 *Appl. Surf. Sci.* **256** 5688

[29] Stanionytė S, Pačebutas V, Čechavičius B, Bičiūnas A, Geižutis A, Bukauskas V, Butkutė R and Krotkus A 2018 *Journal of Materials Science* **53** 8339

[30] Alhassni A, Coelho-Júnior H, Henini M, Gobato Y G and Galeti H V A 2020 *J. Appl. Phys.* **127** 125704

[31] Faria F A, Guo J, Zhao P, Li G, Kandaswamy P K, Wistey M, Xing H and Jena D 2012 *Appl. Phys. Lett.* **101** 032109

[32] Baraskar A, Wistey M, Jain V, Singisetti U, Burek G and Thibeault B 2007 *Technology* **2** (2001) 5–6

[33] Yu A Y C 1970 *Solid State Electronics* **13** 239

[34] Batool Z, Hild K, Hosea T J C, Lu X, Tiedje T and Sweeney S J 2012 *J. Appl. Phys.* **111** 113108